

Heat Minimization in Buildings Through Hydrogel Based Paint: An Overview

N. Anuja^{1*}, K.J. Shivanjini², M.S.B. Mathu Sumitra², S. Brinthaa²

Abstract

Hydrogel based paint focuses on the utilization of hydrogel which is synthesised through cross-linked polymerization reaction and is used as the main raw material for gel-based paint. This study presents the collection of works related to development and characterization of hydrogel-based paints that leverage the unique properties of hydrogels, such as high-water retention, flexibility, and biocompatibility. This work aims to study the current knowledge on hydrogel-based materials, focusing on their synthesis methods, physicochemical properties, and diverse applications. Hydrogel plays an important role in biomedical and civil engineering applications. This study deals with the collection of works related to the physicochemical and mechanical properties of hydrogel along with the changes in it with the addition of different materials.

Keywords: Paint, hydrogel, thermal, insulation, heat-minimization

INTRODUCTION

The effects of climate change and global warming cannot be ignored, which emphasizes the need for sustainability materials and practices in the varied industries. Coatings industries conventionally use paints that are solvent-based but VOC (Volatile Organic Compounds) emitting have caused environmental degradation. Amidst this change towards a better, more sustainable option, researches are being conducted on incorporating hydrogel technology in coating applications. Hydrogels are three-dimensional polymeric networks that can hold large amounts of water; thus, they are used for their unique properties, such as biocompatibility, flexibility, and environmental responsiveness. Hydrogels can be added in unique ways to enhance the self-healing properties of concrete. Several studies focus on using bacterial spores in the form of hydrogels to enhance calcium carbonate precipitation, thereby healing cracks [1, 2]. Another application of bio-based polymers relates to cellulose/PVA as materials for improving freeze-thaw resistance by regulating free water and reducing the effects of expansion stress [3].

*Author for Correspondence

N. Anuja

E-mail: anu_priya1031@yahoo.com

¹Assistant Professor (Senior Grade), Department of Civil Engineering, Mepco Schlenk Engineering College, Sivakasi, Tamil Nadu, India

²UG Student, Department of Civil Engineering, Mepco Schlenk Engineering College, Sivakasi, Tamil Nadu, India

Received Date: January 09, 2025

Accepted Date: April 11, 2025

Published Date: April 22, 2025

Citation: N. Anuja, K.J. Shivanjini, M.S.B. Mathu Sumitra, S. Brinthaa. Heat Minimization in Buildings Through Hydrogel Based Paint: An Overview. Journal of Construction Engineering, Technology & Management. 2025; 15(2): 35–49p.

The development and application of paints engineered to enhance thermal performance and energy efficiency in buildings. Studies focus on passive radiative cooling paints using titanium dioxide (TiO₂) to reflect solar radiation and emit thermal infrared radiation, thereby reducing surface temperatures [4]. Other studies discuss silica aerogel (SA) addition to water-based paints for improved thermal insulation and scrub resistance [5]. Their effectiveness is determined using several tests such as thermal conductivity measurements, reflectance analysis, and accelerated aging tests. These results are part of the continuing research on the development of sustainable and energy-efficient

building technologies. Hydrogel-based paints are very promising solution to the problems associated with conventional coatings. They are water-soluble, making them easy to apply and clean, and they contain pigments and additives in such a way that they form vivid, durable, and even eco-friendly finishes. Bioactive compounds incorporated within the hydrogel can be used to provide additional functionalities such as antimicrobial properties or self-cleaning capabilities, thereby increasing the performance and longevity of painted surfaces.

This study provides an overview of current research in hydrogel-based products, focusing on the synthesis methods, physicochemical properties, and different applications of hydrogels. Based on the knowledge gained on the advancements made in hydrogel technology and their impact on the construction industry, this paper can serve as a means of illustrating the potential of hydrogel-based products as an environmentally friendly alternative to traditional methods [6, 7]. The challenges and limitations in material development and commercialization during the development process will be discussed, which will ensure future research and applications. The role of hydrogel-based products in sustainable development and their contribution to the environment [1, 8].

CHARACTERIZATION OF HYDROGEL

Wang *et al.* studied the sustainability of concrete self-healing by encapsulating bacterial spores in hydrogels and incorporating them into mortar specimens. Healing efficiency tests were performed, which showed that hydrogel-encapsulated spores precipitated CaCO_3 , which was validated by TGA, hence proving the self-healing potential of the mortar. The bacterial spore specimens healed the maximum width of cracks to about 0.5 mm, whereas the non-bacterial specimens healed cracks up to only 0.3 mm. Moreover, the water permeability of the bacterial specimens reduced by an average of 68%, which shows enhanced durability, whereas in non-bacterial specimens, the reduction was between 15 and 55%. This indicates that bacterial spores can substantially enhance the self-healing capabilities of concrete and therefore present a promising approach for the enhancement of the durability and sustainability of concrete structures. The findings indicate potential integration of biological solutions in construction materials with the view of enhancing performance and maintenance [1].

Wu *et al.* explored an innovative method to enhance the freeze-thaw resistance of concrete in cold regions by limiting free water and alleviating expansion stress. This approach involves cross-linking an eco-friendly polymer during freeze-thaw cycles to immobilize free water. The study examines the modification mechanism of the polymer and its impact on the three-dimensional pore structure of hardened cement paste. Results show that incorporating cellulose/PVA hydrogel helps maintain compressive strength after 20 freeze-thaw cycles. The cellulose/PVA solution promotes early hydration of cement without significantly altering the composition of hydration products. After freeze-thaw cycling, the hydrogel network exhibits a multiscale pore structure that effectively reduces osmotic and expansion pressures. Additionally, the hydrogel addition inhibits fracture propagation in hardened cement paste due to freeze-thaw damage. Overall, this method shows promise for improving the durability of concrete in extreme climatic conditions [3].

Vafaei *et al.* studied the effect of hydrogels in improving self-healing behaviour in cementitious systems consisting of high supplementary cementitious material content, slag, and fly ash. Material characterization techniques involved thermogravimetric analysis (TGA), Fourier transform infrared spectroscopy (FTIR), and scanning electron microscopy (SEM/EDS). It was found that in the cement slag system, the healing products mainly were calcium carbonate and hydration products like calcium silicate hydrate and ettringite. On the other hand, the cement fly ash system produced mainly calcium carbonate and C-S-H/C-A-S-H. In addition, the ratio of calcium carbonate to hydration products was found to be greater in the fly ash systems compared to the slag systems. Hydrogels significantly increased the amount of calcium carbonate present in the healing products in both systems. Additionally, incorporation of hydrogels in cement slag and fly ash system led to improved mechanical recovery along with enhanced crack filling relative to the control system where hydrogels were

absent. The results demonstrate that hydrogels do have a positive effect on self-healing potential of cementitious materials [8].

Wang *et al.* addressed the problem in concrete cracking as they researched self-healing concrete encapsulated using bacterial spores. Wang *et al.* synthesized pH-responsive hydrogel designed to condition the spores against some of the harsh conditions in the concrete. It was found that the pH responsiveness of hydrogel, its effects on mechanical properties, and viabilities of spores enclosed within the hydrogel. Results showed that the hydrogel containing chitosan has maintained the stable swelling capacity at pH between 7 and 11 but decreased upon exposure to cement filtrate. Incorporation of the hydrogel at 1 m% resulted in a 5% reduction in compressive strength. Hydrogel-encapsulated spores in specimens significantly decreased water flow (81–90%) and were able to seal effectively all cracks, with over 30% of the crack locations being completely bridged at fracture. Other specimens reached sealing of only 2–12% of crack locations. Overall, the findings have the potential to provide better self-healing for concrete by using pH-responsive hydrogels [2].

Fahimizadeh *et al.* introduced a new strategy to improve biologically self-healing capabilities for sustainable concrete. This includes encasing spores of the *Bacillus pseudofirmus* and yeast extract with halloysite clay nanotubes (HNTs) and then implantation in calcium alginate microcapsules. This encapsulation technique provides protection against the harsh conditions of cement and enhances the interface between the microcapsules and cement, allowing for the retention of nutrients even after exposure to cement pore solutions. The healing system demonstrated remarkable effectiveness in repairing artificial concrete cracks, achieving a reduction in water permeability of over 95%. Further, it showed a mechanical regaining of around 75% after the wet-dry incubation period which was found to be 56 days. The mechanism of releasing the sustained amount significantly led to the enhanced self-healing performance of the concrete that has shown its potential of this approach to improve durability and longevity in concrete structure [9].

Aday *et al.* examined the possibility of non-superabsorbent, thermo-responsive poly (N-isopropyl acrylamide) (PNIPAM) hydrogel particles, with a size of less than 250 μm , for reducing autogenous shrinkage in cement paste and countering the early-age stiffening normally developed with traditional superabsorbent polymers (SAPs). Swelling tests revealed that the early stiffening developed with SAPs was due to its super-absorbent behaviour in low-ionic solutions, a characteristic not present in PNIPAM. The study revealed that 0.3 wt.% PNIPAM addition reduced the autogenous shrinkage strain by 29% at 14 days. In addition, a combination of 0.15 wt.% PNIPAM and 0.15 wt.% SAP resulted in an even greater reduction of about 60% compared to the control. The subsequent series of experiments involved mixing 0.3 wt.% PNIPAM which, relative to the control was reported to decrease autogenous shrinkage by ~29%, and relative to the SAP modified pastes by ~37%. The results indicate non-superabsorbent hydrogels such as PNIPAM can significantly contribute towards the reduction of early age stiffening and induced SAP-related autogenous shrinkage and are thus likely good internal curing agents of cementitious materials [10].

Zhou *et al.* discussed the transparent polyacrylamide/polyvinyl alcohol (PAM/PVA) interpenetrating network hydrogel that improved the durability of the UV irradiation of the fireproof glass grouting. The optimum PVA content was determined to possess strong optical transparency and higher ability to lock water in a grouting fireproof glass compared to PAM only, with 3 wt% PVA having 92.6°C in the backside temperature for 3600 sec while its PAM-only glass resulted in 51.9% less. Thermogravimetric and differential scanning calorimetry analyses indicated improved thermal stability, with the 3 wt% PVA sample achieving a 39.2% residual yield at 800°C. The hydrogel prolonged water evaporation during heat absorption, enhancing flame retardancy. Accelerated aging tests demonstrated that PVA significantly reduced blistering and yellowing. After 168 h of aging, the 2 wt% PVA sample showed only a 19.2°C rise in backside temperature and a 1.9% loss in light transmittance. The PAM/PVA hydrogel generally has great potential to improve the performance of fireproof glass under UV exposure [11].

Zhou *et al.* addressed the critical safety concern of thermal runaway (TR) propagation in lithium-ion batteries (LIBs) by developing a thermally insulating phase change hydrogel with improved mechanical properties. The synthesis mechanism of the hydrogel was clarified through microscopic morphology and elemental analysis. Mechanical tests revealed that the compressive strength increased significantly from 15.58 to 42.87 MPa with the addition of NPG and MMT, allowing the material to endure collisions during TR events. Thermal stability tests showed that the hydrogel effectively absorbs heat generated during TR, emitting only 2.12 g of CO and CO₂, which accounts for 3.98% of total gas emissions. Inhibition studies demonstrated that hydrogel fillers of 2 and 4 mm extended the TR triggering time of adjacent batteries by 294 and 820 sec, respectively, effectively blocking TR in diagonal batteries. Overall, this hydrogel presents an economical, efficient, and environmentally friendly solution for mitigating TR propagation in LIB modules [12].

CHARACTERIZATION OF PAINT

Lai *et al.* discussed the problems associated with the consumption of global energy and the challenges in climate change, particularly the urban heat island effect and the need for efficient cooling systems. They discussed the technology of passive radiative cooling, where the atmospheric window (8–13 μm) is used to emit thermal infrared radiation without additional energy input. The technology reflects solar radiation, while emitting thermal infrared radiation, and hence the surface temperature drops. The study focused on the development of titanium dioxide (TiO₂) cooling paint tailored for Malaysia's tropical climate. The researchers looked into the effects of incorporating Polyvinylidene Fluoride (PVDF) with acrylic as a binder, testing different concentrations to find the optimum composition. The TiO₂ cooling paint outperformed a selected commercial white paint in cooling performance across different surfaces. It demonstrated that the cooling paint averaged a net cooling power of 90.87 W/m² under direct solar irradiation. Besides that, the study focused on determining how weather conditions impact the net cooling power of the paint to support various applications in the urban management of heat [4].

Simpson *et al.* studied the potential of a thin layer of thermal paint with insulating additives to save heating energy in solid wall “hard to heat” housing. The aim of the study was to test energy-saving claims based on a systematic analysis of the material characteristics and thermal performance of various internal coatings using accepted international testing methods. The thermal paint was contrasted with standard coverings such as emulsion paint, wallpapers, and expanded polystyrene liners. A dynamic model of the Energy House research facility was used to make calculations to evaluate energy saving, cost, and payback time. The study concluded that the thermal paint was little better than ordinary vinyl textured wallpapers with lining paper in respect of thermal resistance. The modelling predictions had an unfavourable payback period of several hundred years with a range of energy savings of 0.4–2.9% with the coating thickness and type. Moreover, the scanning electron microscopy results did not support the claims that the additive powder particles were nano-porous or that the coatings had low emissivity surfaces, which would make thermal paint ineffective for energy saving [6].

Lu *et al.* synthesized silica aerogel (SA) powder through a sustainable route using incineration bottom ash. The SA obtained presented low thermal conductivity of 0.025 W/mK, high surface area of 786 m²/g, and high porosity of 96.36%. Thermal analysis presented stable hydrophobicity up to 418°C. The SA powder was used in water-based paints to prepare a high-efficiency thermal insulation paint, called silica aerogel thermal insulation paint, or SATIP. Various percentages of SA were added to the paint samples, and their physical properties were studied systematically. The SATIP showed remarkable improvement in scrub resistance when coated on cement board substrates, and this improvement reached 219% with 5 vol% SA powder. In addition, at 20 vol% SA, the surface temperature decreases up to 12°C when the plate was already heated at 60°C, and the chamber temperature reduces by 1°C from an external temperature of 44.6°C. Spectral reflectance analysis showed that SATIP paint exhibited enhanced thermal insulation due to the properties of SA and confirmed that the paint is colour insensitive, thus suitable for multiple applications. The study shows a low-cost, scalable process for fabricating SA with superior properties, demonstrating SATIP's potential for use in sustainable and energy-efficient buildings [5].

Dias *et al.* studied the influence of cool paints and thermal insulation on the thermal behaviour and energy demand of residential buildings, both old and new constructions. The study made use of the dynamic computer simulator ESP-r to analyse these impacts and give recommendations to designers and homeowners on optimal thermal comfort solutions. In a case study of a building in Portugal, it was found that the increase of TSR of the roof and façade from 50 to 92% reduced maximum indoor free-float temperatures by 2.0 to 4.7°C in old constructions without thermal insulation and by 1.2 to 3.0°C in new constructions with thermal insulation. However, the increase in reflectance was accompanied by a reduction in minimum indoor temperatures of up to 1.5°C. The annual energy demand for heating peaked at about 30% when cool paints were used, while the cooling demand was considerably reduced, and even possibly eliminated, the need for air-conditioning systems. Analysis indicates that the altitude of the sun, which changes month-to-month, is one influence of the effectiveness of cool paints since, as the year progresses and the altitude of the sun decreases, results become better [7].

RESULTS AND DISCUSSION

Figure 1 represents the SEM image of hydrogels with bacterial spores (HAS), after immersion in water and drying. The swelling capacity of pure hydrogels in Deionized Water (DW) is found to be about 14–18 g/g with no significant variation observed between three measurements. Blended hydrogels, HA and HAS, showed lower swelling capacity in the range of 9–11 g/g during the first test, which increased to the range of 20–27 g/g in the second and third tests. This trend shows that blended hydrogels showed a higher swelling capacity than pure hydrogels in later tests [1], which is shown in Figure 2. In filtered cement (FC), pure hydrogels again indicated a higher swelling capacity, about

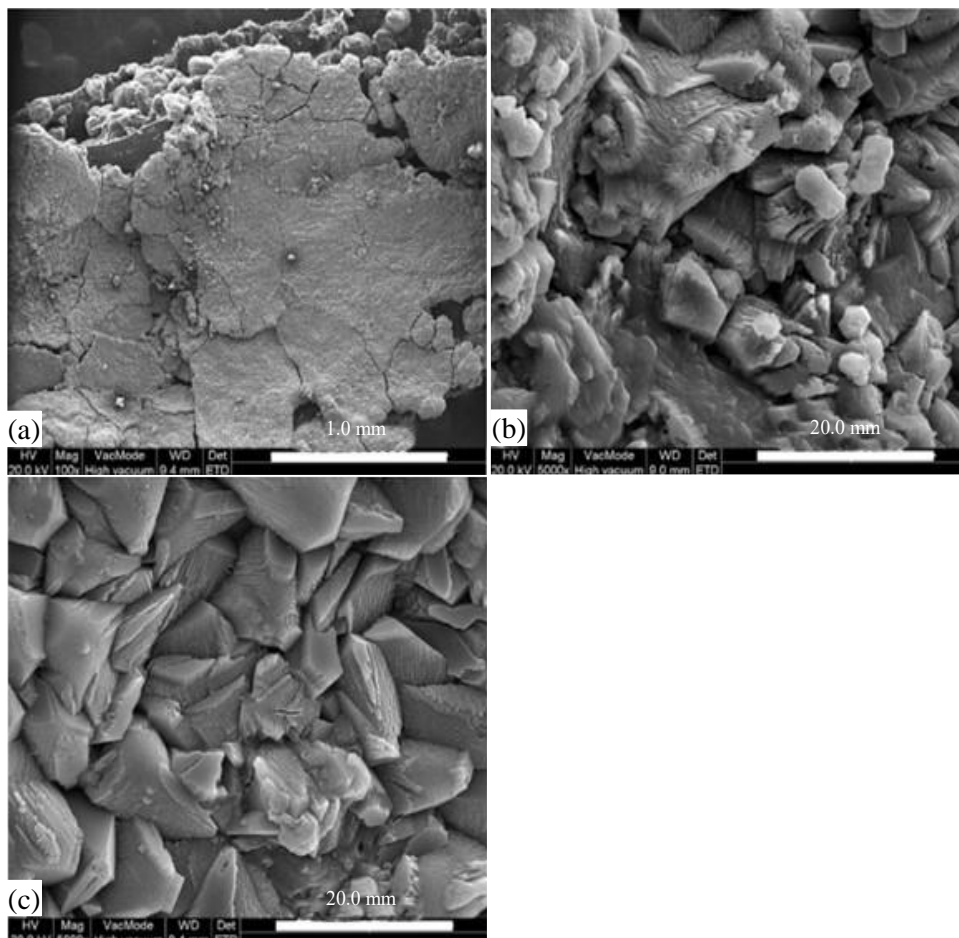


Figure 1. SEM images showing the hydrogels with bacterial spores (HAS), after immersion in water and drying [1].

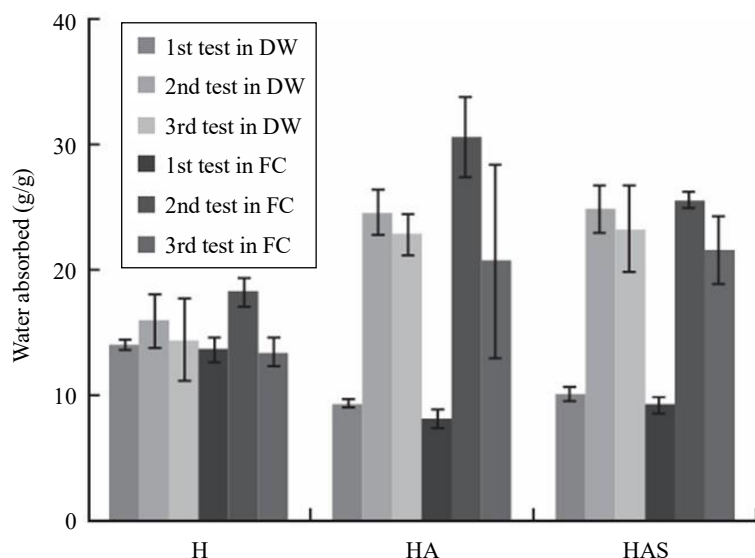


Figure 2. Initial swelling.

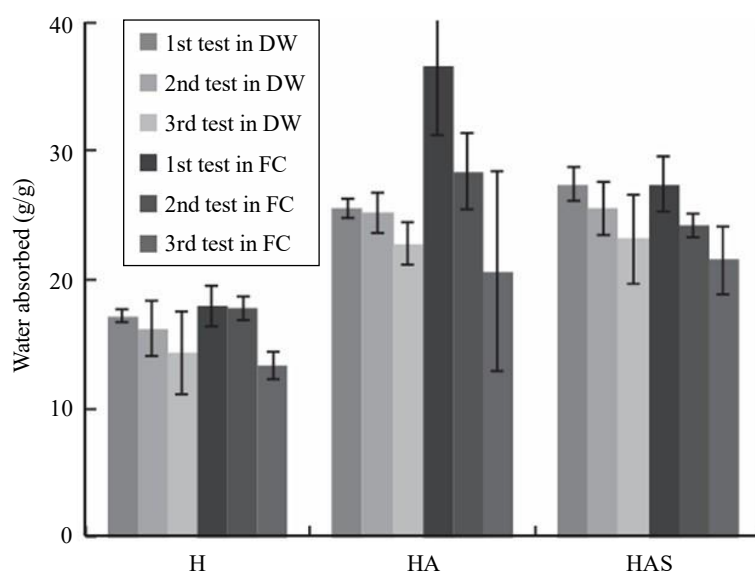


Figure 3. Modified swelling tests results: the amount of the water absorbed in each swelling test was divided by the final dry weight (after 2nd test) of the hydrogels [1].

14 g/g, in the first test, while the blended hydrogels have a capacity of 8–10 g/g. Analogous to the DW results, the swelling capacity of blended hydrogels increased during the subsequent tests. Water absorbed by pure hydrogels was in the range of 14–18 g/g, while blended hydrogels absorbed more, and the range was 19–33 g/g [1]. The results are shown in Figure 3.

A significant weight loss was observed after the first swelling test, especially in the blended hydrogels, with weight losses of about 20% for pure hydrogels and 60% for blended ones. This weight loss mainly occurred after the first test, and after the second test, the weight loss was minimal, showing no significant difference in dry weight between the first and second tests [1]. Due to the considerable weight loss after the first test, the swelling capacity data were recalculated using the dry weight from the second test as the final reference. After recalibration, swelling capacity values for the blended hydrogels increased. The re-calculated swelling properties revealed that blending resulted in a small

increase of the swelling capacity in both DW and FC compared to the pure hydrogels [1]. All the hydrogels presented coherent swelling and re-swelling characteristics in all the performed tests, with both liquids yielding comparable capacities. These imply that the swelling properties were retained irrespective of the test medium [1].

The pure hydrogel can retain absorbed water for up to 48 h with 60% relative humidity at 20°C. After 12 h, about 70% of the absorbed water remained in the hydrogels. The weight of the saturated hydrogel in water continued to go down when exposed to air, and by 48 h, the weight stabilized, and the hydrogel had reached an equilibrium state. After 12 h, about 70% of the water was present, and after 24 h, this amount decreased to 30%. This behaviour shows that the hydrogel is able to retain water over time, though with gradual loss. The hydrogel, demonstrates effective water retention characteristics under specified conditions which is depicted in Figure 4 [3].

The study examines the effects of various hydrogel types on the heat flow rate and cumulative heat release during cement hydration over the first 24 h. It shows that the addition of a cellulose/PVA solution accelerates early cement hydration, especially at a cellulose to PVA ratio of 1:1 and 1:3. The cumulative heat of cellulose/PVA blended cement exceeds that of cement paste. The cellulose/PVA addition modifies the peak release values and timing of hydration. Cellulose fineness has little effect, but the cellulose to PVA ratio significantly impacts early hydration. A 1:1 ratio significantly shortens the acceleration period and advances the main hydration peak, resulting in higher cumulative heat. This indicates that

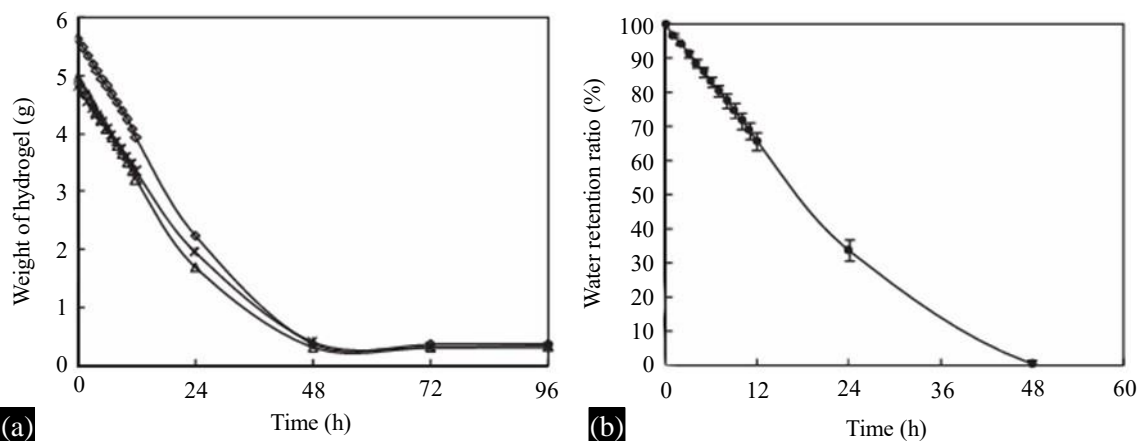


Figure 4. Water retention capacity of the pure hydrogel [3]. (a) Weight changes of the wet hydrogels, (b) Water remaining in the hydrogel.

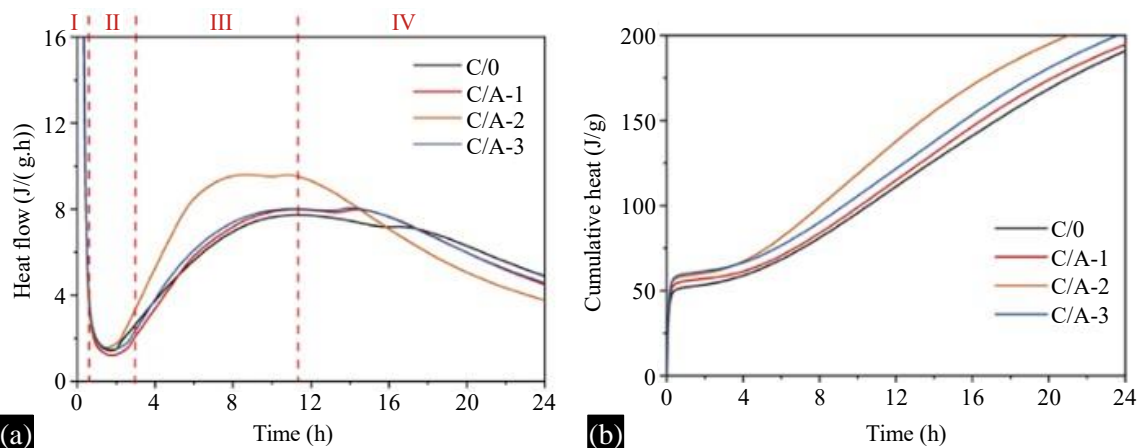


Figure 5. Effect of hydrogel on heat release of cement pastes within 24 h (with 20 μ m cellulose/PVA solution) [3].

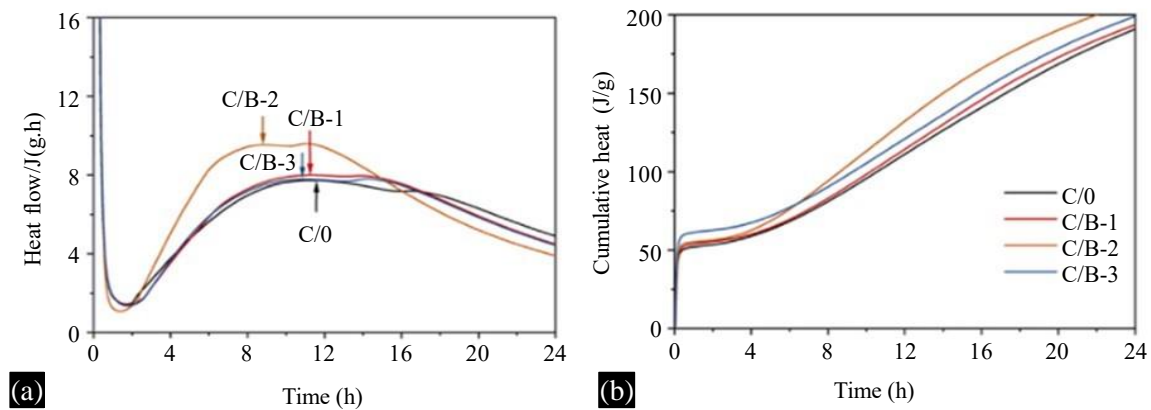


Figure 6. Effect of hydrogel type on heat release of cement paste within 24 h (with 90 μm cellulose/PVA solution) [3].

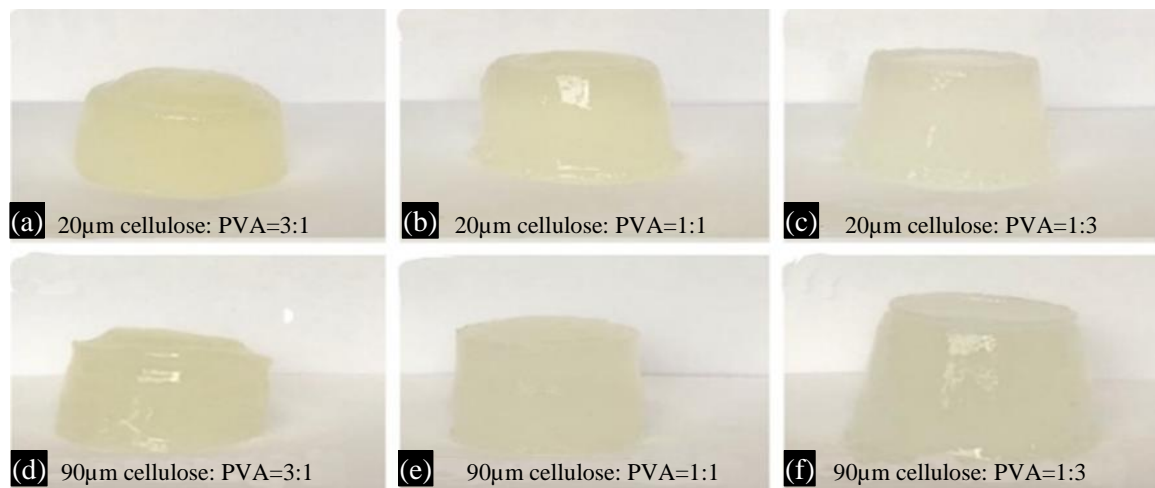


Figure 7. The appearance of hydrogels prepared after freeze-thaw cycling [3].

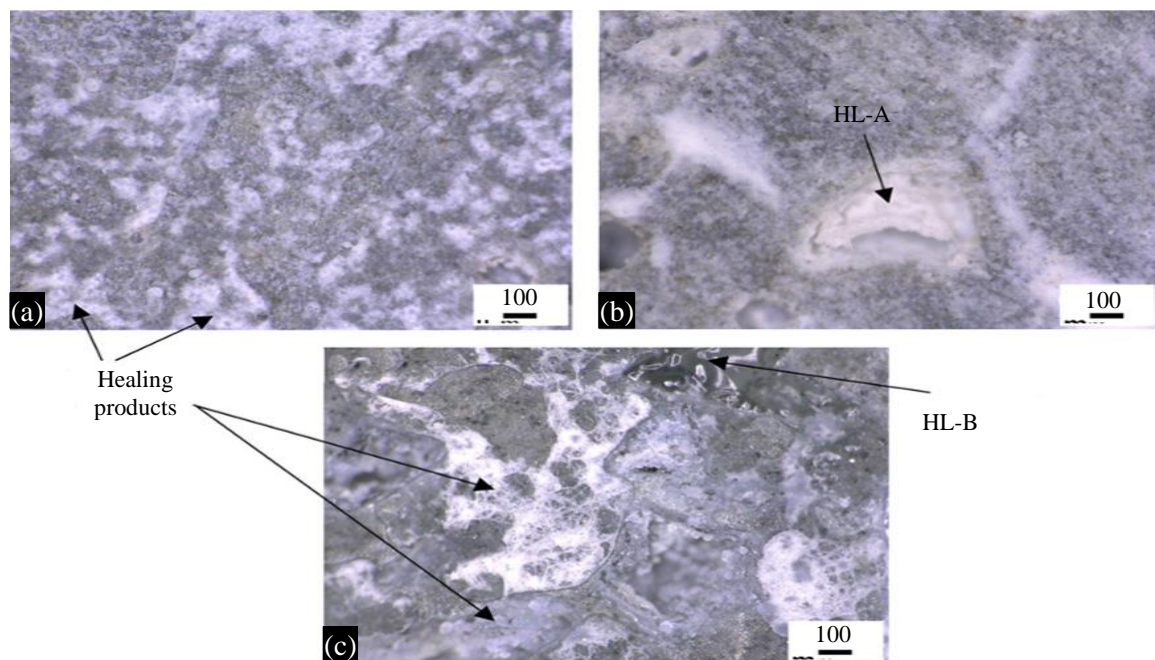


Figure 8. Optical microscopic images of the healing products formed on the artificial crack surface of: (a) S, (b) S-HL-A and (c) S-HL-B [8].

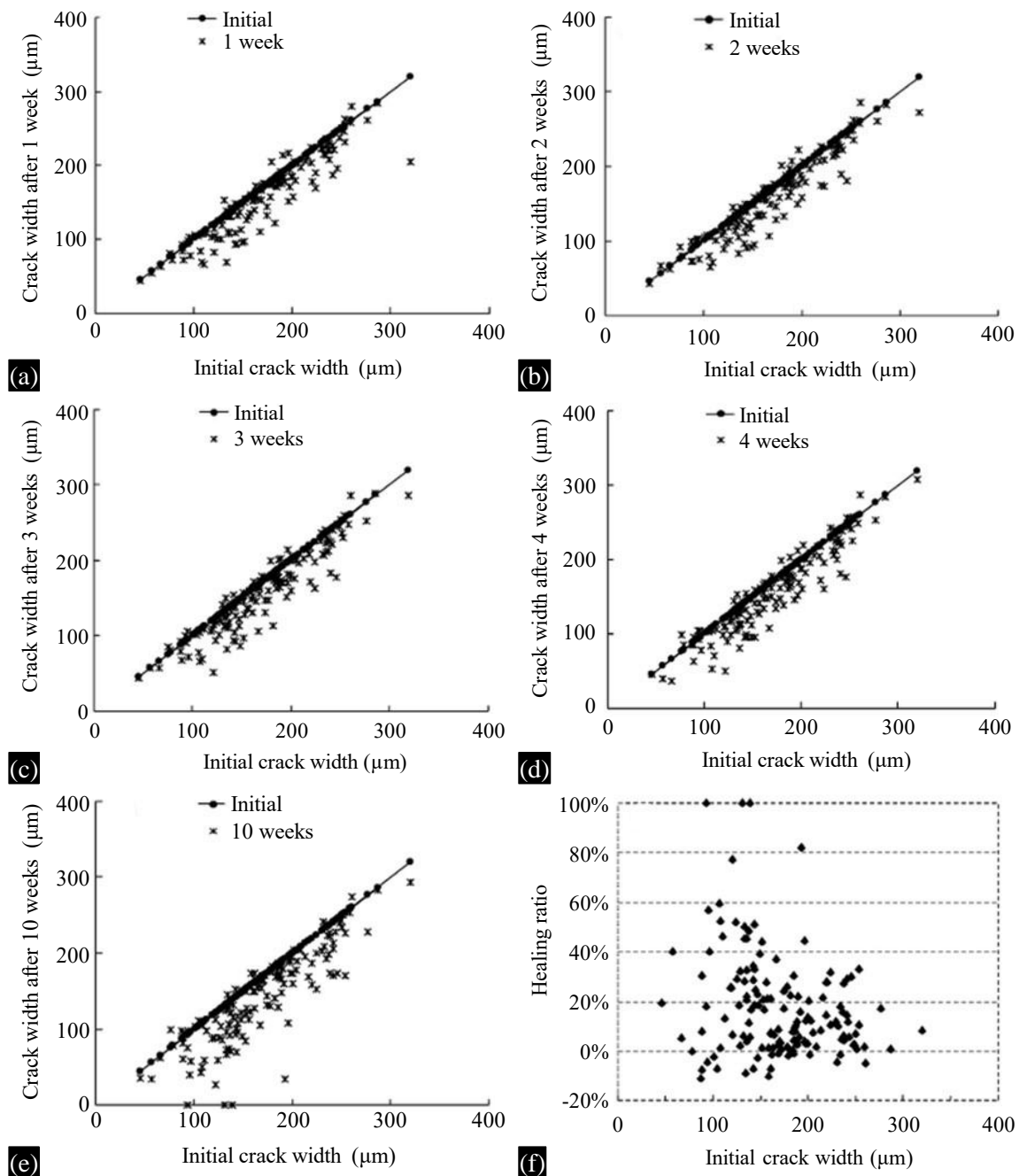


Figure 9. Evolution of crack width (a)–(e) and the sealing ratio for cracks of different widths, (f) in the specimen R [2].

cellulose/PVA addition offers additional nucleation sites for C-S-H growth, which promotes hydration [3]. The picturization of the same have been shown in Figures 5–7. Figure 8 illustrates the healing products (HP) formed on artificial cracks in control slag paste and slag paste modified with HL-A and HL-B. HP is identified as a white substance that partially covers the surfaces of the slag paste. This indicates that healing mechanisms are present in the materials. The additives HL-A and HL-B seem to improve the formation of these healing products. Overall, it demonstrates that these modifications have a great effect towards healing slag paste [8].

Figure 9 indicates the graphical representation of star dots closer to the X-axis represent smaller crack widths and higher healing ratios. After 10 weeks, the R specimens showed limited crack sealing. In the

first week, some star dots moved downward, suggesting a reduction in crack width. However, no significant decreases were observed in the following weeks. By the end of 4 weeks, no cracks were fully closed, and only three locations were completely closed after 10 weeks, which was just 2% of the total investigated locations. Most crack locations showed sealing ratios below 40%. The maximum bridged crack width was around 150 μm , but most small cracks, especially those less than 100 μm , remained unsealed. In some instances, the crack width at the final crack width was larger than that of the initial width. Thus, the sealing ratios came out negative. This indicates the failure to achieve effective crack sealing, particularly for the smaller cracks, and the healing process had very limited effectiveness in terms of overall effectiveness on the R specimens. Thus, some healing occurred but it was not enough to close the cracks fully in most cases [2].

Figure 10 presents infrared spectrum of MMT, SA, CMCS, and hydrogel for thermal insulation. MMT curve has the highest peak around 3621 cm^{-1} from stretching vibration of the Al-OH bond. Two peaks due to bending vibration appear at approximately 825 and 521 cm^{-1} , assigned for Al-Mg-OH and Si-O-Al vibration peaks respectively, proving that the MMT was found within the hydrogel. A common peak around 3350 cm^{-1} in all four curves hints towards O-H stretching vibrations but with decreased intensity in thermal insulation hydrogel possibly through hydrogen bonding between MMT and NPG. Characteristic peaks of the aldehyde acid for SA curves appear at 2924 cm^{-1} due to C-H stretching while the one occurring at 2932 cm^{-1} for hydrogel shows branching in carbon structure. The SA curve also displays a peak at 1591 cm^{-1} due to the stretching of carboxylic acid anion. In the CMCS curve, the peaks at 1585 and 1413 cm^{-1} correspond to the N-H bending vibrations, where the 1585 cm^{-1} peak disappears in the hydrogel because of the electrostatic interactions between CMCS and SA.

The hydrogel curve displays a peak at 1669 cm^{-1} due to C=O stretching, thereby proving the successful incorporation of monomer AA. Moreover, bands at 1559 and 1455 cm^{-1} represent the amide and C-H bending vibrations, respectively. These changes prove the successful grafting of AAM and AA along with the integration of MMT and NPG into a multi-dimensional hydrogel network [12].

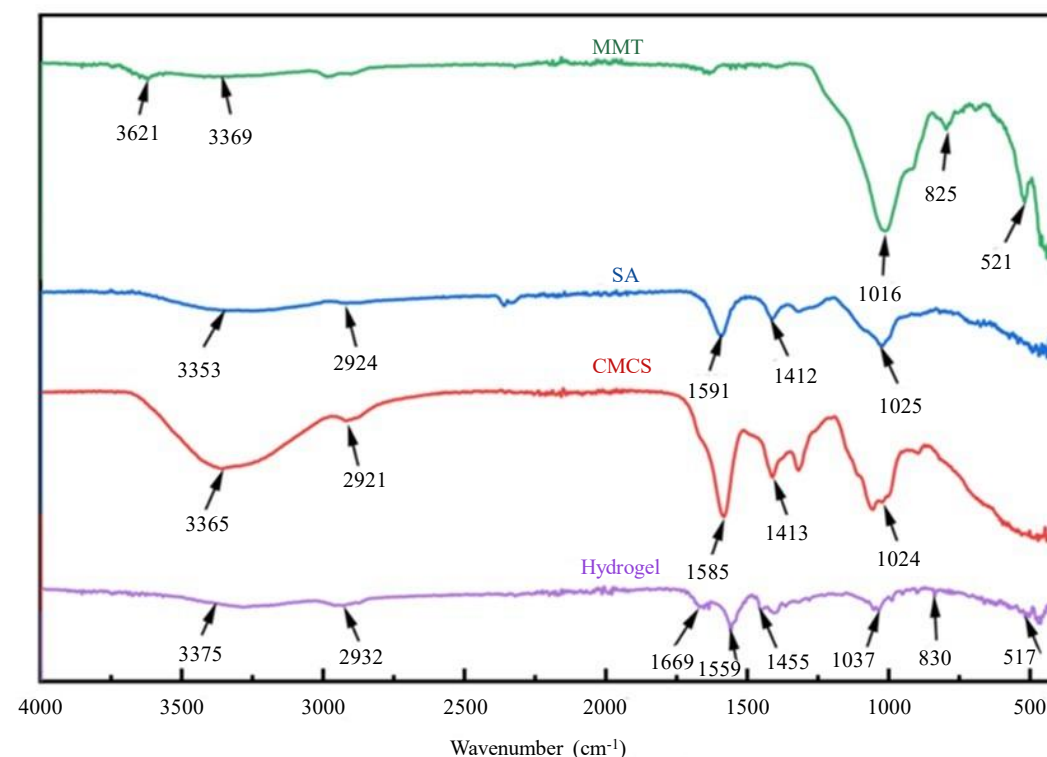


Figure 10. FTIR experiment results of raw materials MMT, SA, CMCS and thermal insulation hydrogel [12].

An interval of 5% concentration difference was applied to a long ceramic tile that was sprayed with pigment. Figure 11 shows the temperature difference between the ceramic tile and ambient temperature at different pigment concentrations. Table 1 summarises the average temperature differences and standard deviations of the data obtained. The ceramic tile has high thermal absorptivity, meaning that it cannot attain sub ambient temperatures, and its temperature is always higher than that of the ambient environment. With increased pigment concentration, the temperature difference between the ceramic tile and ambient temperature decreases. However, 50 wt% TiO₂ achieved the lowest temperature difference from ambient conditions. However, the standard deviation was at its minimum with 45 wt% TiO₂ concentration. It means the data points are highly clustered around the mean value. Therefore, this clustering increases the reliability of the results. Hence, 45 wt% TiO₂ concentration was considered to be optimum composition with balance between the temperature difference and reliability of data. Overall, findings suggest that even though higher concentration reduces temperature difference, the repeatability of results at 45 wt% is a preferred option [4].

SEM observation of the thermal paint coatings indicates that except in Thermal Paint 5 all the samples consist of an embedding of spherical additive particles within a fine irregular shape paint matrix Figure 12(a–e). Thermal Paint 5 is characterized as paintable, sprayable printable paste with the content of an elastomeric polymer incorporating aerogel and glass microspheres as seen from Figure 12(f), it is the sample with rounded up particles between 10 and 100 μm in diameter. There the spheres are agglomerated with an amorphous binder in a semi-continuous form containing very little interparticle matrix material. The microscopic interior morphology of the paint after cutting with a razor blade

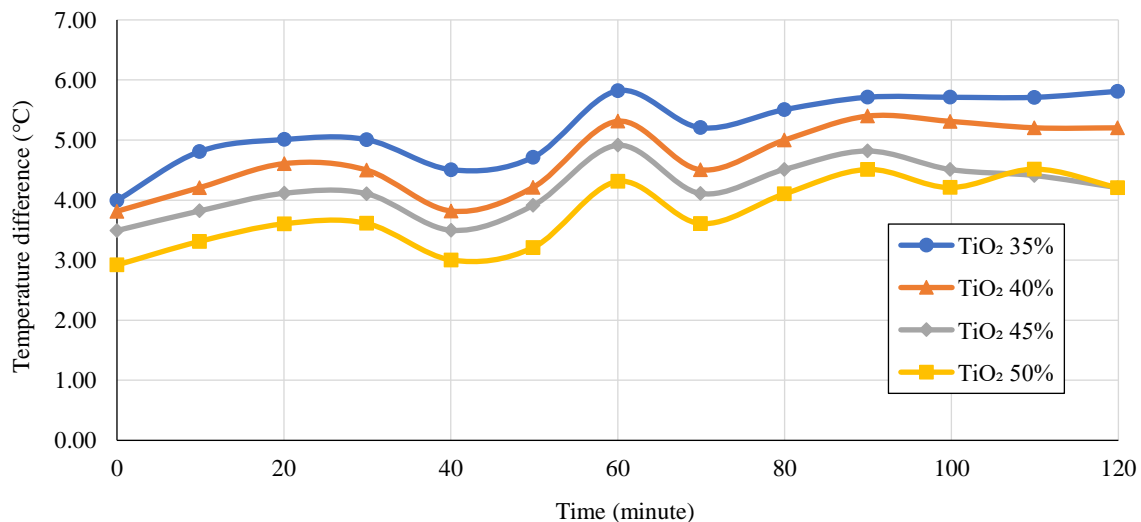


Figure 11. Temperature difference of surface against ambient temperature of TiO₂ at different concentrations [4].

Table 1. Difference in average temperature and standard deviation of specimen with different concentration.

Average temperature difference and the standard deviation of different concentrations		
Concentration	Average	Standard deviation* (%)
TiO ₂ 35 wt%	5.185	0.576
TiO ₂ 40 wt%	4.692	0.578
TiO ₂ 45 wt%	4.177	0.440
TiO ₂ 50 wt%	3.769	0.563

*Standard deviation (%) = $\sqrt{\frac{\sum(\text{Value in data distribution} - \text{Sample mean})^2}{\text{Total number of readings}}}$

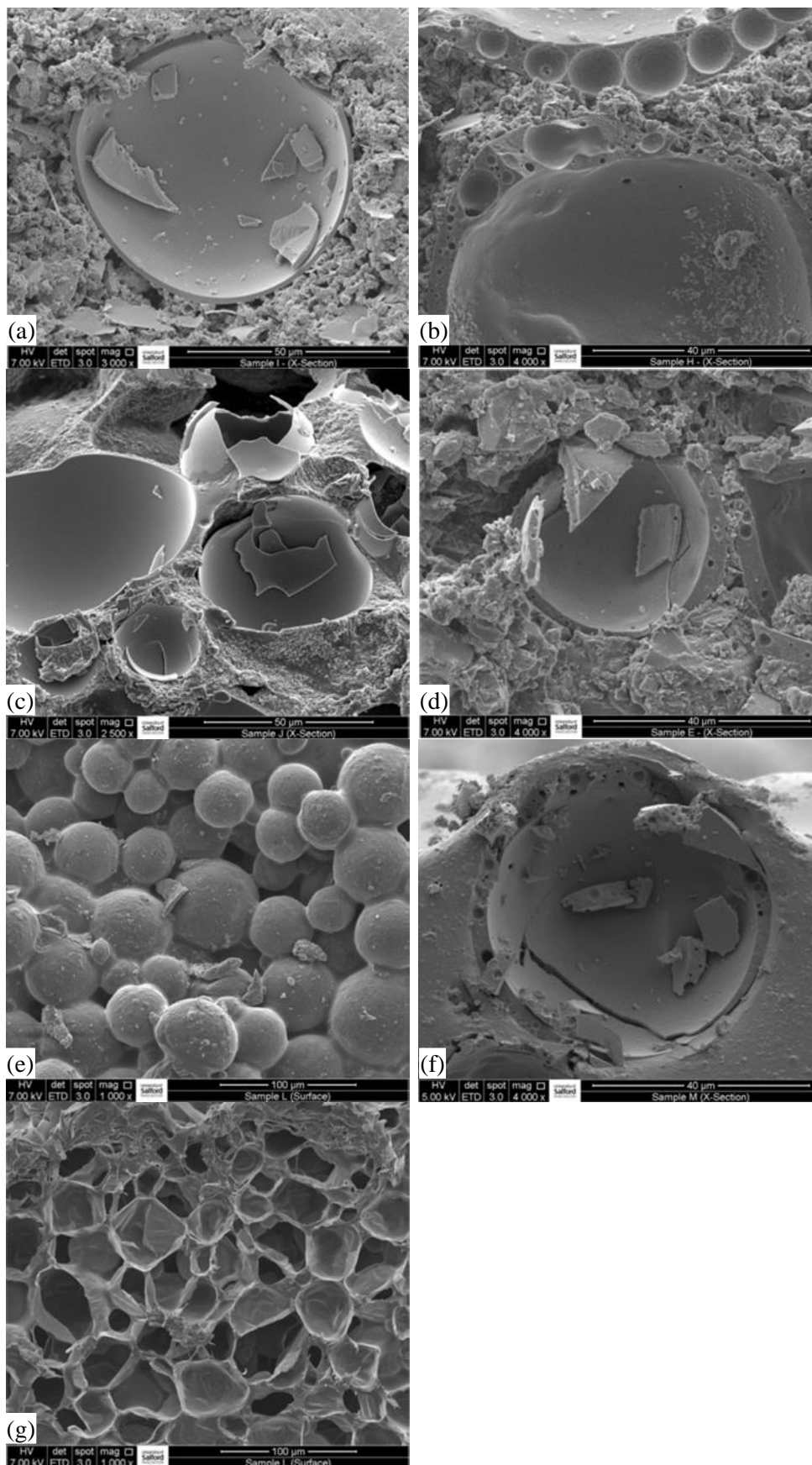


Figure 12. (a)-(g) Thermal paint (1-6).

having been frozen in liquid nitrogen is shown in Figure 12(g). The analysis shows that the spheres are hollow with extremely thin walls, and lots of voids exist between the particles. The spheres are soft and appear to be polymeric rather than ceramic, unlike the earlier samples analysed. The structure of Thermal Paint 5 appears to offer the potential for advantages in the application of thermal insulation due to its lightweight and porous properties. Overall, the results pointed out the distinct morphological features of Thermal Paint 5 compared to other thermal paints.

Figure 13 shows the TGA result of the synthesized SA powder indicating its thermal stability. At 75–125°C, a very small amount of weight loss is present, which might be the evaporation of trapped water, less than 2%. As the temperature moves up to between 375 and 775°C, the weight loss is around 9%. The onset degradation temperature is around 418°C where the SA degrades from oxidation of silicon-carbon bonds (Si-CH_3) to silanol groups (Si-OH), with evaporation of the organic components off the surface. This thermal treatment then changes the initially hydrophobic SA to a hydrophilic variant by substituting the Si-CH_3 groups with polar Si-OH groups along the silicate network. TGA analysis highlights the thermal behaviour and structural changes in the SA powder due to heat exposure. These findings can be observed in Figures 14 and 15 [5].

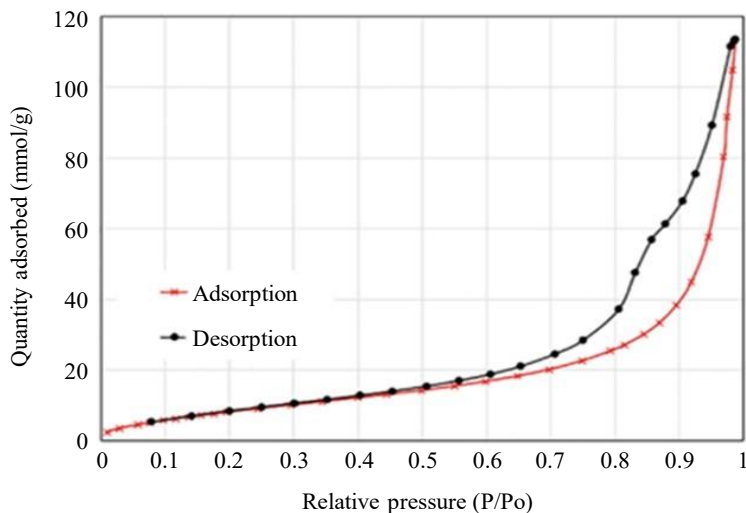


Figure 13. N_2 adsorption and desorption isotherm of fabricated SA powder at 77 K [5].

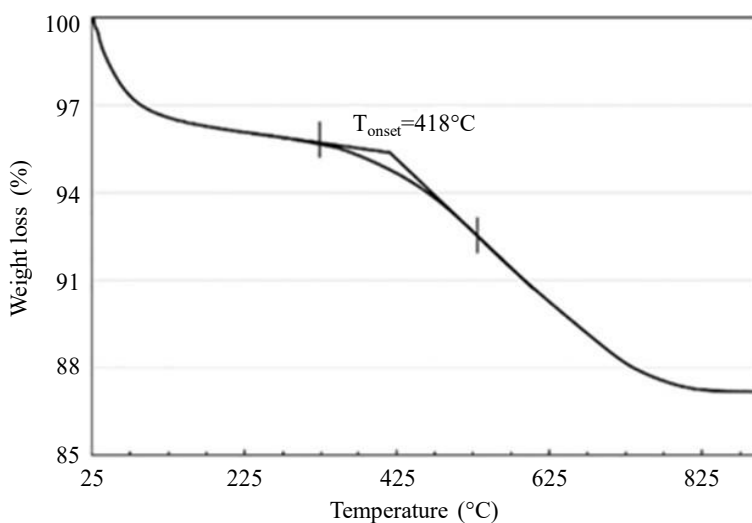


Figure 14. TGA curve for the fabricated SA powder [5].

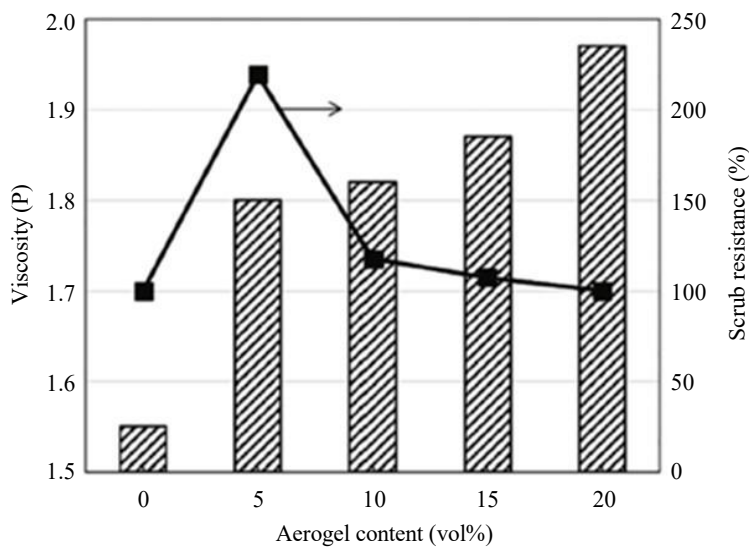


Figure 15. Viscosity of wet paints and abrasion resistance of dry paints with different SA content [5].

CONCLUSION

In this paper, we pay attention to the innovative approaches on the ways of how energy efficiency in construction and enhancement of indoor thermal comfort can be improved. The key findings are as follows:

- Hydrogels that integrate encapsulated bacterial spores and pH responsiveness improve concrete's self-healing and crack sealing properties. Hydrogels prepared with cellulose/PVA enhance freeze-thaw resistance in cementitious systems and further improve the properties by increasing the content of calcium carbonate in the cementitious system.
- Hydrogels with PAM/PVA show better durability of fireproof glass. Thermally insulating phase change hydrogel is used for enhancing the safety and performance of lithium-ion batteries.
- When silica aerogel is used in paint, it provides highly efficient thermal insulation. Similarly, TiO₂ paint synthesized gives a net cooling power of 90.87 W/m².

REFERENCES

1. Wang JY, Snoeck D, Van Vlierberghe S, Verstraete W, De belie N. Application of hydrogel encapsulated carbonate precipitating bacteria for approaching a realistic self-healing in concrete. *Constr Build Mater.* 2024; 68: 110–119.
2. Jianyun Wany, Arn Mignon, Gilles Trenson, Sandra Van Vlierberghe, Nico Boon, Nele De Belie. A chitosan-based pH-responsive hydrogel for encapsulation of bacteria for self-sealing concrete. *Cement Concrete Comp.* 2018; 93: 309–322.
3. Kai Wu, Hao Han, Linglin Xiu, Yun Gao, Zhenghong Yang, Zhengwu Jiang, Geert De Schutter. The improvement of freezing–thawing resistance of concrete by cellulose/polyvinyl alcohol hydrogel. *Constr Build Mater.* 2021; 291: 123274.
4. Darren Jing Yang Lai, Elena Maexin Chua, Apurav Krishna Koyande, Hong WT, Ianatul Khoiroh. Harnessing acrylic-PVDF binders in paint formulation for enhanced passive cooling performance. *Appl Energy.* 2025; 377: 124510.
5. Yanru Lu, Zihe Liu, Xiaodong Li, Xi Jiang Yin, Handojo Djati Utomo. Development of water-based thermal insulation paints using silica aerogel made from incineration bottom ash. *Energy Build.* 2022; 259: 111866.
6. Simpson A, Fittonb R, Rattigana IG, Marshall A, Parr G, Swan W. Thermal performance of thermal paint and surface coatings in buildings in heating dominated climates. *Energy Build.* 2019; 197: 196–210.
7. Diana Dias, João Machado, Vítor Leal, Adélio Mendes. Impact of using cool paints on energy demand and thermal comfort of a residential building. *Appl Therm Eng.* 2014; 65: 273–281.

8. Babak Vafaei, Ali Ghahremaninezhad. Self-healing effect of hydrogels in cement slag and fly ash pastes. *Constr Build Mater.* 2024; 438: 137036.
9. Mohammad Fahimizadeh, Pooria Pasbakhsh, Sui Mae Lee, Joash Ban Lee tan, Raman Singh RK, Peng Yuan. Sustainable biologically self-healing concrete by smart natural nanotube-hydrogel system. *Dev Built Environ.* 2024; 18: 100384.
10. Aday Anastasia N, Matar Mohammad G, Jorge Osio-Norgaard, Srubar III Wil V. Thermo-responsive poly(N-isopropylacrylamide) (PNIPAM) hydrogel particles improve workability loss and autogenous shrinkage in cement paste. *Cement.* 2022; 10: 100049.
11. Longxiadi Zhou, Liang Yi, Long Yan, Zhisheng Xu. Construction of transparent PAM/PVA interpenetrating network hydrogel for designing fireproof glass with superior heat insulation and aging resistance. *J Mater Res Technol.* 2023; 27: 3301–3309.
12. Gang Zhou, Qi Huang, Qi Zhang, Chenxi Niu, Huaheng Lu, Siqi Yang, Yang Liu, Zhikai Wei, Shuailong Li, Yang Kong. Thermal insulation phase-change hydrogel with enhanced mechanical properties for inhibiting thermal runaway propagation in lithium-ion battery module. *J Energy Storage.* 2024; 102: 114102.